Neutron-scattering measurements of wave-vector-dependent hydrogen density of states in liquid water

Khaled Toukan,* Maria A. Ricci,† and Sow-Hsin Chen
Nuclear Engineering Department, Massachusetts Institute of Technology, Cambridge, Massachusetts 02139

Chun-Keung Loong and David L. Price
Intense Pulsed Neutron Source and Materials Science Division, Argonne National Laboratory, Argonne, Illinois 60439

Jose Teixeira
Laboratoire Leon Brillouin, Commissariat a l'Energie Atomique, Saclay, Gif-sur-Yvette, France
(Received 5 October 1987)

Inelastic-neutron-scattering spectroscopy is utilized to probe single-particle excitations as a function of temperature in light and heavy water over an energy range of 50 to 600 meV, covering the librational, bending, and stretch vibrational regions of molecular motion. A computer molecular-dynamics simulation of liquid water based on a simple point-charge model is also carried out to compute the Q-dependent proton density of states $G_s(Q,E)$ for direct comparison with the equivalent quantity deduced from experimental measurements on an absolute scale. The calculated classical density of states is lower than the measured one by a factor of 2, indicating the importance of quantum-mechanical corrections at high-energy transfers. The classical simulation fails to predict a combination band at 525 meV which we attribute to a quantum-mechanical process of simultaneous excitation of the stretch vibrational mode and breaking of the adjacent H—O $\cdots$ H hydrogen bond. The temperature dependence of this band is predicted correctly by a quantum-mechanical calculation using a one-dimensional hydrogen-bond model.

I. INTRODUCTION

The study of the vibrational spectrum of liquid water has been traditionally performed by infrared and Raman scattering spectroscopy.[1-4] The intensity of the Raman bands, being related to the fluctuation of the polarizability tensor of the vibrating molecules, is usually difficult to calculate microscopically, although recently some progress has been made along this direction.[5] Due to this difficulty, an alternative scattering technique for studying the high-frequency vibrations in water needed to be investigated. Neutrons appeared to be a competitive and more direct probe for studying the dynamics of hydrogen atoms because of the spin incoherence in neutron scattering from protons.[6] Furthermore, the dynamic structure factor obtained from neutron-scattering experiments can be directly compared with computer molecular-dynamics (CMD) results. The first attempt to measure the stretch vibration in water and ice by neutron scattering was by Harling[7] in 1968. Due to the low flux of epithermal neutrons in the reactor source he used, the measured stretch vibrational band occurred at a wave-vector transfer Q which is far too large for this excitation to have any appreciable intensity. The energy resolution of the neutron chopper used was also insufficient at this high energy. It was not until a spallation neutron source such as the Intense Pulsed Neutron Source (IPNS) at Argonne National Laboratory came into existence that neutron scattering from high-energy excitations in liquid water became practical.

Previously we have reported preliminary measurements of incoherent inelastic neutron scattering at high energies from liquid water at room and supercooled temperatures.[8] The data, without any multiple-scattering correction, were compared to the proton density of states $f_p(E)$ computed by CMD simulation done at $Q=0$.[9] It appeared from the experimental data obtained that there was a significant contribution of multiple scattering in the measured cross section. The Q dependence of the proton density of states $G_s(Q,E)$ was also quite significant, especially at lower energies. Hence, the comparison between the reported experimental results and CMD calculations could not be made on a quantitative basis.

In this work a thorough analysis of the previous measurements and newly acquired data is presented. Multiple-scattering corrections were made on the measured cross sections and the Q-dependent proton density of states $G_s(Q,E)$ for liquid water at various temperatures is reported in absolute units. The Q-dependent deuteron density of states is also determined for heavy water (D_2O) without accounting for multiple-scattering effects. CMD runs have also been carried out in addition to the experimental measurements to calculate the Q-dependent proton density of states $G_s(Q,E)$ by Fourier transforming the current autocorrelation function $J_s(Q,t)$ and compare it directly with the measured one. The advantage of directly measuring the Q-dependent proton density of states of water and the possibility of direct comparison with CMD calculations are of great value for understanding the dynamics of water. Although there

are numerous CMD simulations for liquid water using various potential models,[10–13] to our knowledge this is the first time that the Q-dependent proton density of states at a high-energy vibrational range covering the intramolecular motion of hydrogen atoms has been computed. This calculation turns out to be essential for understanding the qualitative features of the experimental spectra and indicate the inadequacy of classical CMD simulation for accounting quantitatively for the high-frequency dynamics of water.

An important new feature determined by the measurements is a combination band at 525 meV attributable to a quantum-mechanical process involving a simultaneous excitation of the stretch vibration and breaking of an H bond in liquid water.[14,15] Our recent classical CMD simulation shows only minor features at this energy for any of the Q values calculated, confirming our expectation that this band corresponds to a quantum-mechanical excitation.

II. EXPERIMENT

Neutron-scattering measurements were performed at the high-resolution medium-energy chopper spectrometer (HRMECS) at the Intense Pulsed Neutron Source (IPNS) of Argonne National Laboratory. This spectrometer is particularly well suited for investigations of excitations in liquids at high-energy transfers due to the higher flux of epithermal neutrons available from the pulsed source as compared to conventional reactor sources. The schematics of HRMECS is shown in Fig. 1(a). Since the details of the IPNS chopper spectrometers have been given elsewhere,[16] we shall present only a brief description of the operations here. A phased Fermi chopper produces pulses of monochromatic neutrons incident on the sample. The energy and momentum transfer of the scattered neutrons are determined by time-of-flight techniques in an assembly of 120 detectors. Having a high incident energy E in conjunction with low scattering angles, we are able to measure high-energy excitations at relatively low wave-vector transfers Q where the effect of Doppler broadening is small [Fig. 1(b)]. The energy resolution in general depends on the chopper in use and varies with energy transfer but is approximately 2–4 % of the incident energy [Fig. 1(c)]. In order to calibrate the spectrometer, a run was made using as sample a thin plate of vanadium. Since vanadium is an incoherent scatterer with a well-known scattering cross section,[16] the measured intensity from the detectors was normalized to the vanadium data and put into absolute units of the scattering cross section.

For light water, the time-of-flight spectrum of the neutrons scattered from the sample is essentially the incoherent double-differential cross section of hydrogen atoms, due to the large value of the incoherent cross section of hydrogen compared to that of oxygen. The incoherent double-differential cross section is related to the self-dynamic structure factor $S_s(Q,E)$ for a given wave-vector transfer Q and energy transfer E by

$$\frac{d^2\sigma_{\rm inc}}{d\Omega\, dE}=\frac{N_{\rm H}\sigma_{\rm inc}^{\rm H}}{4\pi\hbar}\left[\frac{E_0-E}{E_0}\right]^{1/2} S_s(Q,E)\ , \qquad (1)$$

where $N_{\rm H}$ is the number of hydrogen atoms in the sample, $\sigma_{\rm inc}^{\rm H}$ is the bound incoherent scattering cross section for hydrogen, and the wave-vector transfer Q (in Å) at a scattering angle ϕ is given by in terms of the incident energy E_0 and energy transfer E (in meV) by

$$Q=0.693(2E_0-E-2\sqrt{E_0(E_0-E)}\cos\phi)^{1/2}\ . \qquad (2)$$

For heavy water, the spectrum contains both coherent and incoherent scattering. However, at large values of Q the interference effects in the coherent scattering should be small and a formula analogous to Eq. (1) should be approximately valid with $\sigma_{\rm inc}^{\rm H}$ replaced by the total scattering cross section σ_T^D.

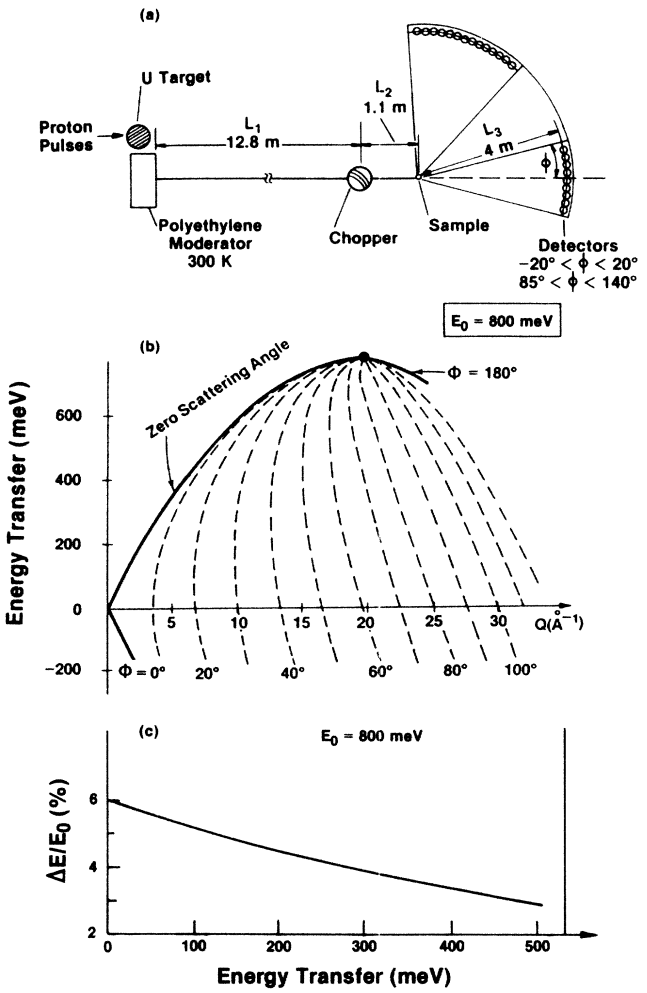

FIG. 1. (a) A schematic diagram of the high-resolution medium-energy chopper spectrometer (HRMECS). The sample-to-detector flight path is 4 m with two groups of neutron detectors spanning angular ranges of $-20°$–$20°$ and $85°$–$140°$. (b) The kinematic relations of the chopper spectrometer at an incident neutron energy $E_0=800$ meV. Energy transfer E (meV) is plotted vs wave-vector transfer Q(Å^{-1}) for different detector angles ϕ ($0°$–$100°$). (c) Energy resolution of the chopper spectrometer as a function of energy transfer E (meV). The energy resolution is less than 4% at the typical energy of the stretch band of water (420 meV).

For liquids, a more convenient quantity to report for direct comparison with CMD calculations is the Q-dependent density of states $G_s(Q,E)$, related to the self-dynamic structure factor $S_s(Q,E)$ by

$$G_s(Q,E)=\frac{E^2}{Q^2}S_s(Q,E)\ . \tag{3}$$

The water sample consisted of an ensemble of 150 thin Pyrex capillary tubes covering an area of 7.2×6.6 cm in planar geometry. The capillary tubes had an inside diameter of 0.8 mm and an outside diameter of 1.0 mm and were filled with triply distilled deionized water and sealed on both ends. The use of Pyrex capillary tubes made it possible to substantially supercool the water. The capillary tubes were mounted on an aluminum frame perpendicular to the incident neutron beam. The incident beam traversed a distance less than 3 mm in the sample for all detector angle ($-15°$–$20°$). This geometric configuration reduced the effect of multiple scattering in the sample. The transmission of the water sample was 84% at an incident neutron energy of 500 meV. To keep the sample temperature as uniform as possible, the ensemble of capillary tubes was enclosed in a thin-walled aluminum container filled with helium gas. A helium cryogenic refrigerator was employed for the low-temperature runs and a vacuum furnace was used for measurements at elevated temperatures. The temperature was controlled to an accuracy of 0.5 °C.

Measurements were made on ice at 20 K and on supercooled water at -15 °C with both 800 and 500 meV incident energies. Runs were made at higher temperatures (40 °C and 80 °C) at 800 meV only. For heavy water (D_2O), measurements were carried out at -93.4, and 25 °C at an incident neutron energy of 500 meV. To confirm that the H_2O sample at -15 °C was indeed liquid, a separate measurement was performed under identical conditions at the crystal analyzer spectrometer at IPNS, where the quasielastic peak could be measured with much higher resolution. In the case of ice, the width of this peak corresponded to the instrumental resolution (135 μeV), whereas at -15 °C it was appreciably broader (230 μeV), indicating the characteristic diffusion of the liquid state; the value obtained for the width agrees well with the results of a triple-axis measurement on supercooled water.[17]

III. DATA REDUCTION AND MULTIPLE-SCATTERING CORRECTIONS

Multiple-scattering effects were simulated by running Copley's MSCAT routine[18] for both filled and empty containers. In the main Monte Carlo loop, the history of 40 000 incident neutrons has been traced. Scattering events were detected at ten different scattering angles in the range $2°$–$20°$. Since the MSCAT routine allows for only one row of cylinders, an effective sample geometry (50 tubes, 0.171-cm external radius, 0.0342-cm thickness, and 0.377-cm center-to-center distance) was used. The number of scattering units in the simulated sample matches that of the water molecules in the real sample. As an input to the MSCAT routine, a reasonable symmetrized scattering function $\tilde{S}_s(Q,E)$ is needed for the Monte Carlo simulation. Starting from the density of states $f_p(E)$, evaluated by molecular-dynamics simulation,[9] $\tilde{S}_s(Q,E)$ was calculated by means of a modified version of Copley's SABMAK routine.[18] The calculation of $\tilde{S}_s(Q,E)$ assumes the incoherent, monatomic, cubic, harmonic approximation for one- and two-phonon terms, while third- and higher-order phonon terms are calculated according to a modification of Sjolander's theory.[19] The low-energy region of $f_p(E)$ was modified according to the one-phonon harmonic approximation. The Debye-Waller factor was evaluated by assuming a root-mean-square displacement[20] of 0.484 Å.

The MSCAT routine accumulates separately single- and multiple-scattering contributions. In the present case, multiple scattering from the container is negligible. In contrast, multiple scattering from the sample is structureless and increases with energy transfer. It accounts for approximately 50% of the total scattered intensity at energy transfers greater than 500 meV.

The experimental data were corrected for multiple-scattering effects and self-shielding and sample-attenuation factors (SSF and SAF) by means of the MULCOR routine,[21] which has been recently improved to predict the SSF for both slab and cylinder geometries. For the water sample, the SSF and SAF have values of 65% and 95%, respectively. The corrected time-of-flight data have been interpolated to generate constant-E or constant-Q plots. The Q-dependent density of states is depicted in Figs. 2 for light water at temperatures of -15, 40, and 80 °C in absolute units of (meV Å^2) after making multiple-scattering corrections. The prominence of the combination band at 525 meV at lower temperatures is clearly noted. The corresponding data for heavy water at temperatures of -93, 4, and 25 °C is shown in Fig. 3. Multiple-scattering corrections were not made in this case, however, due to the lack of CMD data on the proper deuteron density of states.

IV. COMPUTER MOLECULAR-DYNAMICS SIMULATION (CMD)

The intermolecular potential model employed in this CMD is the simple point-charge model originally proposed by Berendsen *et al.*[22] The potential consists of a pairwise Lennard-Jones interaction between the oxygen sites, $v_{00}=-(A/r)^6+(B/r)^{12}$ with $A=0.371\,22$ nm(kJ mol^{-1})$^{1/6}$ and $B=0.3428$ nm(kJ mol^{-1})$^{1/12}$, together with Coulomb interactions between suitable point charges at the oxygen and hydrogen sites. We assign a change $+0.41|e|$ to each hydrogen site and $-0.82|e|$ to the oxygen site. The intramolecular potential is an anharmonic Morse function for the O—H bond and a harmonic function for the H-H interaction. Internal coupling between the two O—H bonds, as well as coupling between the stretching and bending modes, has also been inserted in the potential,

$$V_{\rm mol}=D_{\rm OH}\{[1-\exp-(\rho\Delta r_1)]^2+[1-\exp(-\rho\Delta r_2)]^2\}+\tfrac{1}{2}b\Delta r_3^2+c(\Delta r_1+\Delta r_2)\Delta r_3+d\Delta r_1\Delta r_2\ . \tag{4}$$

Here, $\Delta r_1, \Delta r_2$ are the stretch in the OH bond lengths and Δr_3 is the stretch in the H-H distance. The parame-

ters D_{OH}, ρ, c, and d are taken with a small modification from Toukan and Rahman[9] with $D_{OH}=0.708$ mdyn/Å, $\rho=2.37$ Å^{-1}, $b=2.283$ mdyn/Å, $c=-1.469$ mdyn/Å, and $d=0.776$ mdyn/Å. The system we studied consisted of 100 molecules in a constant-volume simulation cell with periodic boundary conditions. CMD runs at a density of 1 gm/cm^3 and temperature $T=250$ K were made with a time increment $\Delta t=6.5\times10^{-16}$ sec. The system was aged for several thousand time steps to ensure reaching thermal equilibrium, and the pair correlation functions were checked to see that the correct static structure was generated in the simulation.

Due to the large incoherent scattering cross section of hydrogen atoms as compared to oxygen, inelastic neutron scattering from water primarily measures proton dynamics. We shall focus our attention on the following single-particle current-density autocorrelation function $J_s(Q,t)$ defined as

$$J_s(Q,t)=\frac{1}{Q^2}\left\langle\frac{1}{N}\sum_{j=1}^{N}[\mathbf{Q}\cdot\mathbf{v}_j(t+\tau)][\mathbf{Q}\cdot\mathbf{v}_j(\tau)]\times\exp\{i\mathbf{Q}\cdot[\mathbf{r}_j(t+\tau)-\mathbf{r}_j(\tau)]\}\right\rangle_\tau , \quad (5)$$

where $\mathbf{v}_j$ and $\mathbf{r}_j$ refer to the velocity and the position of the jth proton in the system. The $\mathbf{Q}$ vector in Eq. (5) is sampled from the relation $\mathbf{Q}=2\pi/L$ $(\mu,\nu,\delta=0,\pm,\pm2,\ldots)$, where L is the length of the cubic simulation cell. The choice of the Q values as given above is a consequence of the periodic boundary conditions imposed on the simulation cell. The scalar quantity $J_s(Q,t)$ in Eq. (5) is obtained by averaging over all possible orientations of the momentum transfer $\mathbf{Q}$ for a given Q value. Three different finite Q values of 4.36, 8.72, and 13.08 Å^{-1} were considered. Thirty orientations of the wave vector $\mathbf{Q}$ for a given Q value were considered for $Q=4.36$ and 8.72 Å^{-1} and 150 orientations for $Q=13.08$ Å^{-1}.

The Fourier transform of the current autocorrelation function $G_s(Q,E)$ can be shown to be related to the proton self-dynamic structure factor, $S_s(Q,E)$ by[23]

$$G_s(Q,E)=\frac{h}{\pi}\int_0^\infty J_s(Q,t)\cos\omega t\,dt=\frac{E^2}{Q^2}S_s(Q,E) . \quad (6)$$

From a practical point of view $G_s(Q,E)$ is a natural quantity to calculate for the high-frequency modes of proton motions because the low-frequency part of $S_s(Q,E)$ is attenuated by the factor E^2/Q^2. This leads to

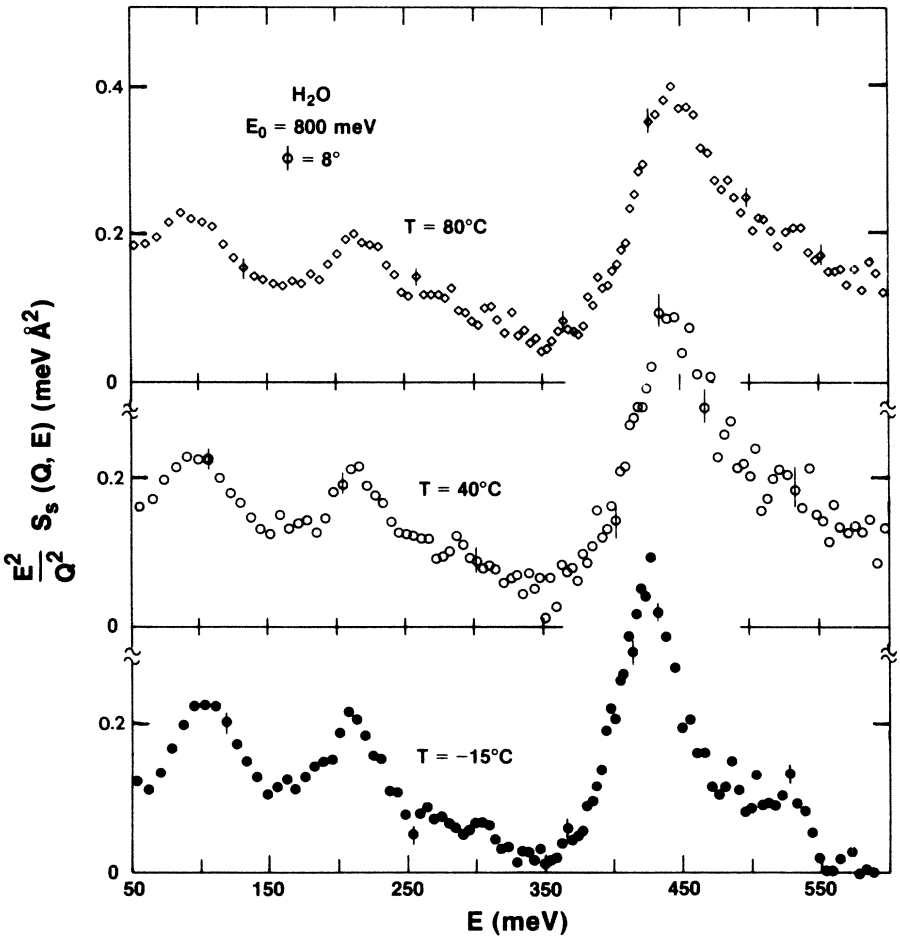

FIG. 2. Q-dependent proton density of states $G_s(Q,E)$ for liquid water (H_2O) at three different temperatures -15, 40, and 80 °C measured by incident neutrons of energy $E_0=800$ meV at a detector group with an average angle $\phi=8°$. Multiple-scattering corrections have been made and the data reduced to an absolute cross section in units of (meV Å^2).

a rapid decay of the time correlation function $J_s(Q,t)$, which allows the Fourier transform of this function to be computed from relatively short histories. Furthermore, since $\lim_{Q\to 0} J_s(Q,t)=\langle \mathbf{v}_H(0)\cdot\mathbf{v}_H(t)\rangle$ and $\lim_{Q\to 0} G_s(Q,E)=f_p(E)$, the quantities $J_s(Q,t)$ and $G_s(Q,E)$ are natural finite-Q extensions of the proton velocity autocorrelation and the density-of-states functions. Several preliminary test runs of CMD showed that the current autocorrelation function $J_s(Q,t)$ decays to 1% of its initial value in less than $600\Delta t$. A trajectory with a minimum of 2000 time steps was used to obtain a good average for the time correlation function at the different Q values. Time correlations were calculated over 1200 time-step periods. The time origin was shifted by 20 steps and this shifting of the origin was done 40 times within each step. The time correlations for the different Q orientations were then averaged to produce the final autocorrelation function which was then Fourier transformed to obtain the proton density of states. Figure 4 shows a plot of this function at four different Q values for direct comparison with experimental data. The density of states is given in units of (meV Å^2) which is the same as that obtained by neutron scattering.

V. DISCUSSION

The Q-dependent proton density of states for liquid water as measured by neutrons of incident energy $E_0=800$ meV is shown in Fig. 2 for supercooled water at a temperature of -15 °C and water at 40 and 80 °C. The spectra show four major bands: a librational band due to intermolecular coupling at an energy of 74 meV, two intramolecular bands, one due to bending at an energy of 207 meV and the other due to stretching at an energy of 418 meV, in addition to a fourth combination band at an energy of 525 meV. The typical nominal wave-vector transfers Q at these bands are 2.8, 3.75, 6.5, and 8.4 Å^{-1} for the librational, bending, stretch, and combination bands, respectively, at a scattering angle $\phi=8°$. The spectrum shown is a depiction of the averaged Q-

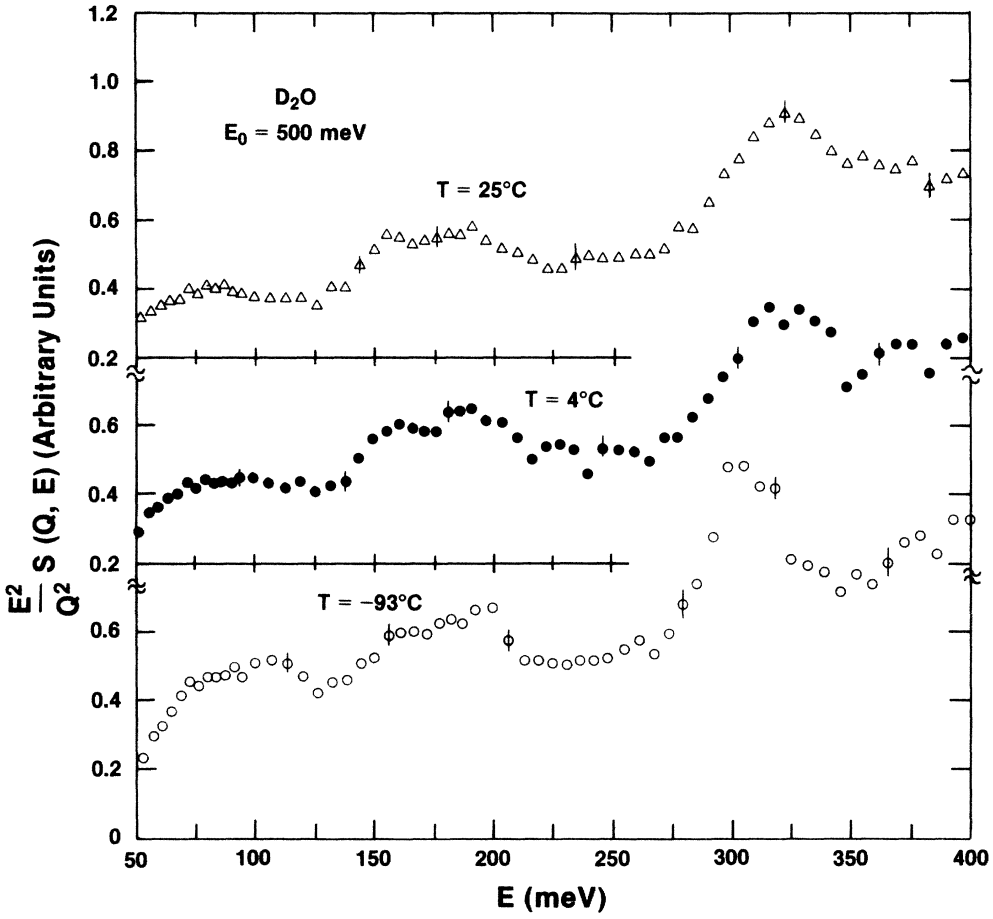

FIG. 3. Q-dependent deterium density of states $G_s(Q,E)$ for heavy water (D_2O) at three different temperatures -93, 4, and 25 °C measured by incident neutrons of energy $E_0=500$ meV averaged over six detector groups spanning an angular range of 4° to 20°. Data have been reduced to an absolute cross section in units of (meV Å^2) but the multiple-scattering corrections have not been made. In the ordinate we use $S(Q,E)$ as the symbol for the dynamic structure factor because, in principle, the coherent scattering is measured for the D_2O case. However, in the large-Q region the dynamic structure factor is practically equal to the self-dynamic structure factor $S_s(Q,E)$.

dependent density of states reduced from the time-of-flight data collected in the detector group at an average angle $\phi = 8°$. At each energy-transfer value E of the abscissa, the corresponding wave-vector transfer Q is given by Eq. (2). The density of states is given in absolute units of (meV Å^2) after making the appropriate multiple-scattering corrections to the self-dynamic structure factor $S_s(Q,E)$ and then converging it into the Q-dependent density of states according to Eq. (3). A peak shift of the stretch vibrational energy band to higher energies as the temperature is increased is noted. This behavior is attributed to the formation of more intact hydrogen bonds between neighboring molecules at lower temperatures which tends to soften the intramolecular attractive bond.[9] A peak intensity increase at lower temperatures is also clearly noted. This is due to quantum-mechanical effects which are very sensitive to temperature and wave-vector transfer of the specific peak. The combination band around 525 meV is also seen to be strongly temperature dependent, becoming sharper and increasing in center energy as the temperature is lowered to that of the supercooled state. This effect can also be explained quantum mechanically. We will separately discuss the temperature variation of both the stretch and combination bands at the end of this section.

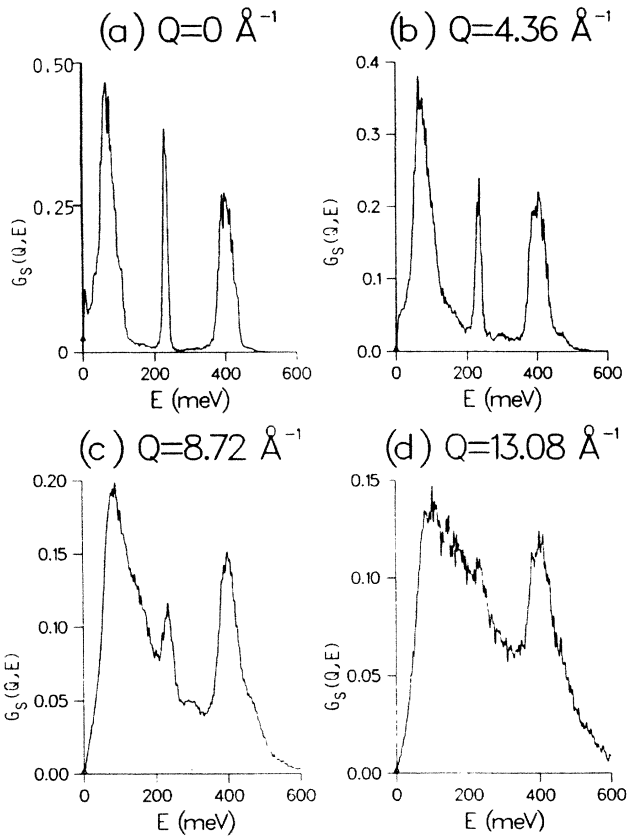

FIG. 4. Q-dependent proton density of states $G_s(Q,E)$ calculated by CMD simulation a temperature of 250 K for Q values of 0, 4.36, 8.72, and 13.08 Å^{-1}. The absolute cross section calculated by the classical CMD simulation is lower by a factor of 2 as compared to that measured experimentally. The spectrum also does not show the combination band at 525 meV indicating the quantum-mechanical origin of the excitations in liquid water.

The corresponding Q-dependent density of states for heavy water (D_2O) is depicted in Fig. 3; as discussed in Sec. III, multiple-scattering corrections have not been incorporated in these data. The main features of the spectrum are the same as those of light water with all bands shifted down in energy by a factor of $\sqrt{2}$ due to the heavier mass of deuterons as compared to that of protons. Although the quality of the data in the D_2O case is not as good as in the H_2O, it can be seen from Fig. 3 that the Q-dependent density of states is considerably more structured in the intermediate energy range.

A computer molecular-dynamics simulation was also performed in addition to the experimental measurements to interpret the experimental results. The simulated spectra at constant Q values predict quite correctly the main features of the measured experimental spectra for light water. Doppler broadening of the librational band at the higher Q values is clearly evident. This feature would not have been observed without carrying out a simulation at finite Q such as the present one.[9] The detailed study of the Q-dependent effect in the librational band should be a matter of further interesting experimental investigation. The simulation also shows a general decrease in intensity due to the Debye-Waller factor at higher Q values. However, direct comparison of the intensity obtained by classical CMD simulation with the corresponding experimental spectra in the stretch region (Fig. 5) indicates that the simulated intensity is lower by a factor of 2 as compared to the experimental spectrum. Furthermore, the CMD spectrum shows only a weak combination band at 525 meV at any of the Q values considered. This discrepancy can only be accounted for by considering a quantum-mechanical excitation in liquid water at these temperatures and confirms earlier calculations which attributed the combination band to this feature.[14,15]

Due to the large number of neutron detectors employed in this experiment, spanning an angular range of $-20° < \phi < 20°$,[2] it was possible to interpolate the time-of-flight data collected in the different detector groups to generate plots for the self-dynamic structure factor $S_s(Q,E)$ at constant Q and then convert it to the Q-dependent density of states for liquid water. Figure 5(a) shows a typical plot for the librational and bending bands at $Q = 7$ Å^{-1}. It is interesting to observe in this constant-Q representation a third band at 280 meV which appears to be a combination band due to coupling between the librational and bending bands. The corresponding plot for the stretch band at a Q value of 10 Å^{-1} is shown in Fig. 5(b). This representation is of importance because of direct accessibility for comparison with CMD data which are usually obtained at constant Q.

The previous discussion clearly indicates that a quantum-mechanical correction of some kind has to be made on the classical simulation results. The prediction of the fourth combination band at 525 meV has already been verified by Ricci and Chen[15] by employing a one-dimensional quantum-mechanical hydrogen-bond model. These authors have been able to account correctly for the

measured energy band in both intensity and band center. The question now is how to correct for the classical CMD simulation to predict the measured experimental intensities for the other three bands in the spectrum. We will focus our attention here specifically on the stretch band because it could be considered the closest to a harmonic oscillator, although it was shown previously that the intramolecular O—H bond is clearly anharmonic in nature[9] as deduced by the energy shift of the stretch band as water changes phase from gas to liquid. Taking a harmonic oscillator model as a first approximation to the real behavior of the stretch vibrational band, one can adopt the rigorous quantum corrections already derived for such systems. Yip and Boutin[24] have worked out the following formulas to correct the classical self-dynamic structure factor to account for the quantum-mechanical effects:

$$S_s(Q,E)=\exp(E/2kT)\exp[-\tfrac{1}{2}\gamma(0)Q^2]S_s^{\mathrm{cl}}(Q,E) \tag{7a}$$

and

$$\gamma(0)=(3kTh/m)\int_0^\infty dE f_p(E)[\cosh(E/2kT)-1]/E^2 , \tag{7b}$$

where m is the neutron mass and $f_p(E)$ is the proton density of states which can be easily generated by CMD simulation. This correction factor consists of a product of a detailed balance factor $\exp(E/2kT)$ and a Debye-Waller-type factor $\exp[-\gamma(0)Q^2/2]$. The first factor is sensitively dependent on temperature T and the latter factor on the square of the wave-vector transfer Q^2.

Although the previously mentioned correction is strictly derived for a harmonic oscillator, we have tested it for the stretch band in water. Equations (7) gives a rather reasonable factor for correcting the calculated self-dynamic structure factor as compared to the experimental one. As an example, for room-temperature water the

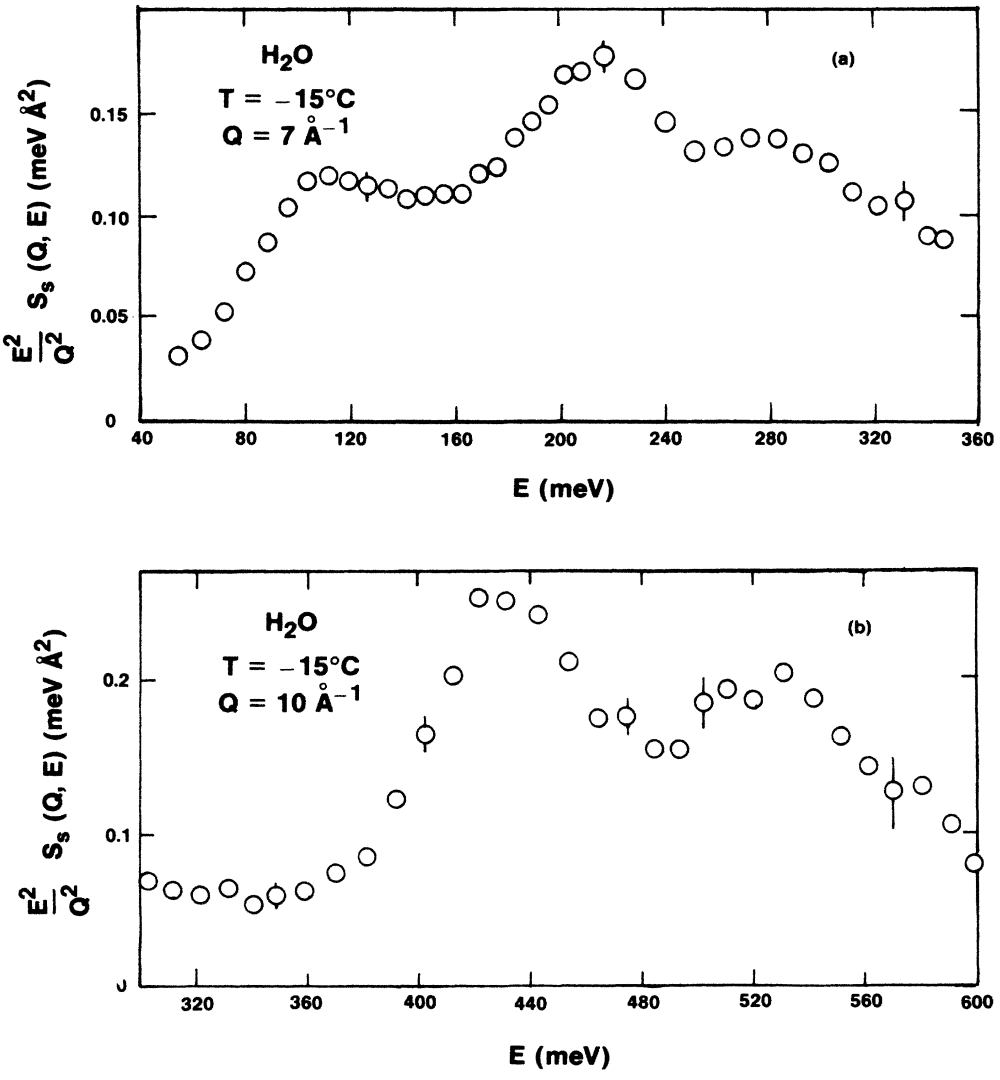

FIG. 5. (a) The measured constant Q density of states in supercooled water showing the librational and bending bands at a Q value of 7 Å^{-1}. (b) The measured constant Q density of states in supercooled water showing the stretch and combination bands at a Q value of 10 Å^{-1}.

attenuation coefficient $\gamma(0)$ is calculated to be equal to 0.21 Å^2 from the CMD data.[25] At a nominal Q value of 8.5 Å^{-1}, stretch band energy center E of 420 meV and temperature of 298 K, the detailed balance factor is about 4200 and the Debye-Waller-type factor 1/2000. Thus, the quantum-mechanical correction factor is equal to 2.1. This value is of the same order of magnitude to account for the difference between the measured experimental and the classical CMD-simulated spectra. However, we have noted that such a correction is very sensitive to temperature T and wave-vector transfer Q, since relatively high-energy transfers E are involved.

There does not exist at present a rigorous, systematic quantum-mechanical correction that can be applied to the whole calculated CMD spectrum of water to match it to the experimental data. Separate models have been worked out in this respect for the stretch and combination bands and agree quite reasonably with the measured experimental data. However, a more thorough quantum-mechanical CMD simulation for liquid water seems to be the most reasonable approach to account for all aspects of the experimental spectrum. It should be remarked here that the successful observation of the stretch vibrational band at an energy of 420 meV by neutron scattering depends on two fortunate aspects. First, it turns out from the classical CMD simulation that the Q dependence of the stretch vibrational band is remarkably small. Second, the quantum-mechanical correction at such a high energy turns out to be a factor much greater than unity, especially at the supercooled temperature.

Referring to Fig. 5(b), a combination band clearly appears in the high-energy region of the Q-dependent density of states of liquid water. A peak at about the same energy position has already been detected in the Raman spectrum of room-temperature water[26] and assigned to the overtone of the librational and stretch bands on the basis of frequency shift analysis. Recently,[14,15] we proposed a quantum-mechanical model involving a one-dimensional hydrogen bond which allows us to calculate the neutron-scattering cross section for the excitation of the stretch vibration with the simultaneous breaking of the H bond in supercooled water. This model accounts for the presence of such a combination band and predicts the correct ratio between the peak intensities of the stretch and combination bands. In the model it turns out

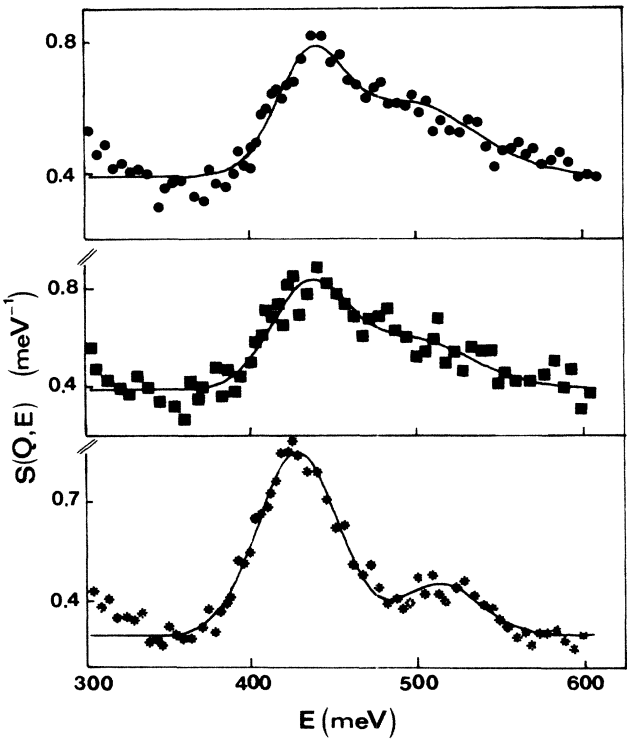

FIG. 6. The incoherent dynamic structure factor $S_s(Q,E)$ showing the stretch and combination bands for liquid water (H_2O) at three temperatures, -15,40,80 °C, together with the best fit at $T=-15$ °C (*): 40 °C (■); and 80 °C (●).

that the combination peak energy and shape are directly related to the mean strength and distribution of the H bond.

In Table I we report the least-squares fit parameters for the self-dynamic structure factor in the region 300–650 meV at $Q=11$ Å^{-1} for three temperatures shown in Fig. 6. The fit procedure takes into account the instrumental resolution ($\sim$24 meV in this energy range). The experimental data at all temperatures we considered can be fitted directly by two Gaussian functions, one for the stretch band (denoted by subscript 1) and the other for the combination band (denoted by subscript 2).

From Table I, one notes that at the higher temperatures all the fit parameters are approximately the same

TABLE I. Least-squares-fit parameters for $S_s(Q,E)$ in the region 300–600 meV at $Q=11$ Å^{-1} for three different temperatures. A_1 and I_1 are the peak and integrated intensity, respectively. W_1 is the full width at half maximum.

T (K)	258	313	353
A_1	0.61±0.02	0.43±0.13	0.37±0.05
E_1 (meV)	428.07±0.77	434.76±3.84	436.91±1.65
W_1 (meV)	51.36±2.14	46.93±10.54	41.04±5.79
I_1	33.51±1.50	21.56±5.5	16.12±2.5
A_2	0.17±0.02	0.21±0.03	0.23±0.01
E_2 (meV)	514.56±2.91	494.52±25.50	496.01±8.89
W_2 (meV)	52.46±8.50	86.13±41.37	91.97±16.37
I_2	9.44±1.60	19.36±9.60	22.42±4.1

within the fitted accuracy. On the contrary, the fitted parameters for supercooled water are substantially different from the others. This behavior indicates that, on going from the supercooled state to room temperature, a strong modification occurs in the H-bond network.

According to our perturbative analysis,[14,15] the energy shift of the combination band is a linear function of the mean value of the hydrogen-bond strength D_2. In this calculation, we chose $D_2=3$ kcal/mole$=130$ meV/molecule, according to a previous spectroscopic estimate.[27] On the other hand, D_2 can be evaluated from the experimental values of the band energy E_2 (combination band) by the following expression:[15]

$$E_2=(430.24+79.98D_2/130)\ \text{meV} . \quad (8)$$

Under this hypothesis, D_2 is evaluated to be equal to 3.2 ± 0.1 kcal/mole for supercooled water and $2.5\pm$ kcal/mole for room-temperature water.

The O—H stretch softening observed in going down to the supercooled state cannot be accounted for by increasing D_2 since the dependence of band energy E_1 (stretch band) on D_2 is less than 1% according to our model,[15]

$$E_1=(430.24-3.09D_2/130)\ \text{meV} . \quad (9)$$

This suggests that the downshift of the stretch band center energy in the supercooled state is mainly due to interactions with the neighboring molecules in the surrounding liquid.

Moreover, the integrated intensities of the stretch and combination bands, denoted by I_1 and I_2 in Table I, can be evaluated by the least-squares-fit parameters. The softening of the hydrogen-bond mean strength observed above room temperature gives rise to a strong increase of the combination band peak intensity while decreasing that of the stretch band.

The intensities I_1 and I_2 can be related to the number P of intact bonds and to the number $1-P$ of broken bonds, respectively. A reasonable evaluation of P is given by $P=1.8-0.004T$.[28] The calculations show that, indeed, the ratio I_1/I_2 agrees with the ratio $P/(1-P)$ to better than 10%, giving additional support to our interpretation of the physical meaning of these two bands.

Finally, we want to stress that the evidence of a relevant modification in the hydrogen-bond network at room temperature can also be observed in the pressure behavior of the viscosity coefficient,[29] and has recently been observed by low-frequency light scattering experiments.[30] In our opinion, the behavior of the integrated intensity of the combination band supports the present interpretation of it as arising from the excitation of the stretch vibration with the simultaneous breaking of the H bond. We think that a more careful study of the D_2O spectrum and more investigations of the details of the librational region in both H_2O and D_2O at various temperatures should be sufficient to distinguish between our interpretation of the combination band and its assignment as an overtone of the librational band.

VI. CONCLUSION

We have presented a quantitative experimental determination of the Q-dependent hydrogen density of states for liquid water at three different temperatures including a supercooled state. These results can be considered to be the state-of-the-art measurements for water using neutron-scattering techniques at the present time. This was possible only because of the availability of the pulsed neutron source which provides an abundance of epithermal neutrons at the HRMECS. A multiple-scattering correction to the measured self-dynamic structure factor has been carried out so that it was possible to compare the Q-dependent density of states directly with CMD data in the case of H_2O. The comparison showed that, for high-energy excitations in water, the quantum-mechanical correction to the classical CMD simulation results is essential. We also identify a new excitation band which is entirely missing in the simulation results. Because of the light mass of hydrogen atoms, it seems that a complete quantum-mechanical CMD simulation of water is necessary in order to interpret the entire features of the experimental spectrum.

ACKNOWLEDGMENTS

We wish to acknowledge the guidance and inspiration of the late Aneesur Rahman during the early stages of the computer simulation. We are grateful to the IPNS staff at Argonne National Laboratory for giving access to the HRMECS spectrometer and providing the needed epithermal neutron beam time. The measurements presented in this paper are the result of three years of collaborative efforts between three groups, involving the use of ten weeks of HRMECS beam time. The Massachusetts Institute of Technology (MIT) group is very grateful to Professor Raman Bansil of Boston University for providing sufficient computer time to carry out the CMD simulation. K.T. is thankful to IPNS for providing financial support during his numerous stays at ANL. M.A.R. acknowledges joint financial support of NATO and Consiglio Nazionale delle Ricerche. The research work of the MIT group is supported by a grant from the National Science Foundation. IPNS and the work at Argonne National Laboratory are supported by the U.S. Department of Energy under Contract No. WP-31-109-ENG-38.

*Permanent address: College of Engineering and Technology, University of Jordan, Amman-Jordan.

†Permanent address: Dipartimento di Fisica, Università di Roma "La Sapienza," Piazzale Aldo Moro, 00185 Rome, Italy.

[1]A review by G. E. Walrafen, in *Water: A Comprehensive Treatise*, edited by F. Franks (Plenum, New York, 1971).

[2]G. D'Arrigo, G. Maisano, F. Mallamace, P. Migliardo, and F. Wanderligh, J. Chem. Phys. **75**, 4264 (1981).

[3]R. Bansil, J. Wiafe-Akenten, and J. L. Taaffe, J. Chem. Phys. **76**, 2221 (1982).

[4]Y. Yeh, J. H. Bilgram, and W. Kanzig, J. Chem. Phys. **77**, 2317

(1982).
[5]R. Bansil, T. Berger, K. Toukan, M. A. Ricci, and S. H. Chen, Chem. Phys. Lett. **132**, 165 (1986).
[6]W. Marshall and S. W. Lovesey, *Theory of Thermal Neutron Scattering* (Oxford, Clarendon, 1971); *Neutron Scattering*, edited by D. L. Price and K. Sköld (Academic, New York, 1987), Part B, Vol. 23.
[7]O. K. Harling, in *Neutron Inelastic Scattering* (International Atomic Energy Agency, Vienna, 1968), Vol. 1, p. 507.
[8]S. H. Chen, K. Toukan, C. K. Loong, D. L. Price, and J. Teixeira, Phys. Rev. Lett. **53**, 1360 (1984).
[9]K. Toukan and A. Rahman, Phys. Rev. B **31**, 2643 (1985).
[10]M. Wojcik and E. Clementi, J. Chem. Phys. **84**, 5970 (1986); **85**, 3544 (1986); **85**, 6085 (1986).
[11]J. J. Ullo, Phys. Rev. A **36**, 816 (1987).
[12]A. Rahman, F. H. Stillinger, and H. L. Lemberg, J. Chem. Phys. **63**, 5223 (1975).
[13]F. H. Stillinger, Adv. Chem. Phys. **31**, 1 (1975).
[14]M. A. Ricci, S. H. Chen, D. L. Price, C. K. Loong, K. Toukan, and J. Teixeira, Physica B **136**, 190 (1986).
[15]M. A. Ricci and S. H. Chen, Phys. Rev. A **34**, 1714 (1986).
[16]D. L. Price, J. M. Carpenter, C. A. Pelizzari, S. K. Sinha, I. Bresof, and G. E. Ostrowski (unpublished); also J. R. D. Copley, D. L. Price, and J. M. Rowe, Nucl. Instrum. Methods **107**, 501 (1973); C. K. Loong, S. Ikeda, and J. M. Carpenter, *ibid.* **260**, 381 (1987).
[17]S. H. Chen, J. Teixeira, and R. Nicklow, Phys. Rev. A **26**, 3477 (1982).
[18]J. R. D. Copley, Comput. Phys. Commun. **7**, 289 (1974); **9**, 53 (1975); **20**, 453 (1980); **21**, 431 (1981).
[19]A. Sjolander, Ark. Fys. **14**, 315 (1958).
[20]J. Teixeira, M. C. Bellissent-Funel, S. H. Chen, and A. J. Dianoux, Phys. Rev. A **31**, 1913 (1985).
[21]J. R. D. Copley, D. L. Price, and J. M. Rowe, Nucl. Instrum. Methods **107**, 501 (1973).
[22]H. J. C. Berendson, J. P. M. Postma, W. F. van Gunsteren, and J. Herman, in *Intermolecular Forces*, edited by B. Pullman (Reidel, Dordrecht, 1981).
[23]S. H. Chen and S. Yip, Phys. Today **29**, 32 (1976).
[24]H. Boutin and S. Yip, *Molecular Spectroscopy with Neutrons* (MIT, Cambridge, MA, 1968).
[25]J. Anderson, Ph.D. thesis, Masschusetts Institute of Technology, 1986.
[26]G. E. Walrafen and L. A. Blatz, J. Chem. Phys. **59**, 2646 (1973).
[27]C. J. Montrose, J. A. Bucaro, J. Marshall-Coakley, and T. A. Litovitz, J. Chem. Phys. **60**, 5025 (1974).
[28]H. E. Stanley and J. Teixeira, J. Chem. Phys. **73**, 3404 (1980).
[29]D. EIsenberg and W. Kauzmann, *The Structure and Properties of Water* (Oxford University, London, 1969).
[30]V. Mazzacurati and P. Benassi, Chem. Phys. **112**, 147 (1987).